Influence of stress and strain on the kinetic stability and phase transitions of cubic and pseudocubic Ge-Sb-Te materials

Matthias N. Schneider,[1] Philipp Urban,[1] Andreas Leineweber,[2] Markus Döblinger,[1] and Oliver Oeckler[1,*]
[1]*Department of Chemistry and Biochemistry, Ludwig Maximilian University Munich, Butenandtstrasse 5-13 (D), D-81377 Munich, Germany*
[2]*Max Planck Institute for Metals Research, Heisenbergstrasse 3, D-70569 Stuttgart, Germany*
(Received 25 November 2009; revised manuscript received 8 February 2010; published 6 May 2010)

Rewritable data-storage media and promising nonvolatile random-access memory are mainly based on phase-change materials (PCMs) which allow reversible switching between two metastable (amorphous and crystalline) modifications accompanied by a change in physical properties. Although the phase-change process has been extensively studied, it has not been elucidated how and why the metastable crystalline state is kinetically stabilized against the formation of thermodynamically stable phases. In contrast to thin-film investigations, the present study on bulk material allows to demonstrate how the cubic high-temperature phase of GeTe-rich germanium antimony tellurides (GST materials) is partially retained in metastable states obtained by quenching of bulk samples. We focus on compositions such as $Ge_{0.7}Sb_{0.2}Te$ and $Ge_{0.8}Sb_{0.13}Te$, which are important materials for Blu-ray disks. Bulk samples allow a detailed structural characterization. The structure of a multiply twinned crystal isolated from such material has been determined from x-ray diffraction data ($Ge_{0.7}Sb_{0.2}Te$, $R3m$, $a=4.237$ Å, $c=10.29$ Å). Although the metrics is close to cubic, the crystal structure is rhombohedral and approximates a layered GeTe-type atom arrangement. High-resolution transmission electron microscopy (HRTEM) on quenched samples of $Ge_{0.8}Sb_{0.13}Te$ reveal nanoscale twin domains. Cation defects form planar domain boundaries. The metastability of the samples was proved by *in situ* temperature-dependent powder diffraction experiments, which upon heating show a slow phase transition to a trigonal layered structure at ca. 325 °C. HRTEM of samples annealed at 400 °C shows extended defect layers that lead to larger domains of one orientation which can be described as a one-dimensionally disordered long-periodical-layered structure. The stable cubic high-temperature modification is formed at about 475 °C. Powder diffraction on samples of $Ge_{0.8}Sb_{0.13}Te$ with defined particle sizes reveal that the formation of the stable superstructure phase is influenced by stress and strain induced by the twinning and volume change due to the cubic → rhombohedral phase transition upon quenching. The associated peak broadening is larger for small crystallites that allow relaxation more readily. Consequently, the degree of rhombohedral distortion as well as the appearance of superstructure reflections upon annealing is more pronounced for small crystallites. The same is true for samples which were slowly cooled from 500 °C. Hence, the lattice distortion accompanying the phase transition toward a stable trigonal superstructure is, to a certain degree, inhibited in larger crystallites. This kinetic stabilization of metastable states by stress effects is probably relevant for GST phase-change materials.

DOI: 10.1103/PhysRevB.81.184102 PACS number(s): 81.30.Hd, 61.50.Ks, 61.66.Fn

I. INTRODUCTION

Rapid data storage using phase-change recording media and nonvolatile random-access memory is a key technology. The phase-change materials (PCMs) involved have to meet the basic requirement that a reversible phase transition between two structurally different phases is related to a change in physical properties.[1–4] For all materials under development, this phase change is based on the transition between amorphous phases and metastable crystalline phases with simple average structures.[5,6] The metastability of the phases that contribute to the write-erase cycle is essential in order to reversibly induce the phase change that allows to code information in solid state. According to the phase diagrams, all materials that are currently used exhibit corresponding thermodynamically stable states, either as additional modifications or involving phase separation.[7–10] The stable compounds do not contribute to the data-storage process but present an energetical minimum which is disadvantageous for the phase-change behavior. Since they must be avoided, it is essential that the kinetic stabilization of metastable phases is sufficient to allow reliable data-storage cycles over long periods. On the other hand, they must allow for fast phase change. Numerous investigations have attempted to elucidate the mechanism of the transition used for data storage,[11–14] however, it remains unclear why the systems under investigation do not reach the thermodynamic equilibrium during their application.

Most studies have focused on alloys in the system Ge-Sb-Te (GST materials).[15] Concerning many analytical methods, it is a drawback that the metastable phases are not easily accessible by solid-state synthesis, but mostly have to be prepared as thin films, e.g., by magnetron sputtering. The crystalline phases in the system Ge-Sb-Te can be classified according to their structures. A rocksalt-type (B1) lattice with Te atoms occupying the anion site and Ge/Sb sharing the cation site has been reported for metastable crystalline phases occurring in the phase-change cycle.[3,16,17] Their composition generally lies on or very close to the pseudobinary section $GeTe\text{-}Sb_2Te_3$ in the ternary phase diagram, where normal valence compounds are located. Thus, a varying content of cation vacancies is intrinsic as there are more Te

atoms than Ge and Sb atoms in this AB structure. The vacancy distribution has been discussed in detail.[3,11,16,18,19] A statistical distribution as well as partial defect ordering two-dimensional arrays have been reported based on DFT calculations.[17,20,21] For both models, local distortions accompany the vacancies.

For GeTe-rich samples obtained by scraping off thin films produced by sputtering, it has recently been shown that the metastable "cubic" B1-type phases, in fact, exhibit a slight rhombohedral distortion.[22] Comparable to pure GeTe,[23] a stable undistorted cubic high-temperature modification does exist; the transition temperature between the rhombohedral and the cubic phases increases with rising GeTe content. Furthermore, a B1-type crystalline phase Ge_4SbTe_5 (=$Ge_{0.8}Sb_{0.2}Te$), has been described,[15,24–26] this composition point slightly deviates from the compositions corresponding to the pseudobinary GeTe-Sb_2Te_3 line.

However, at low temperatures these modifications are metastable: reaching the thermodynamic equilibrium involves phase separation. For example, annealing the metastable phase $Ge_8Sb_2Te_{11}$ ($GeTe:Sb_2Te_3=8:1$) leads to separation into GeTe and a phase with composition $Ge_6Sb_2Te_9$ ($GeTe:Sb_2Te_3=6:1$), which, under these conditions, is probably the ternary phase with the lowest Sb content.[22] It exhibits a long periodically ordered structure which is representative for a range of phases $(GeTe)_n(Sb_2Te_3)_m(Sb_2)_k$. These ordered compounds can exhibit surprisingly large translation periods. They include homologous series of antimony-rich antimony tellurides ($n=0$) (Refs. 27–29) and stable compounds with $k=0$ that contain rigid rocksaltlike building blocks of alternating Te and Ge/Sb layers.[28,30,31] For n, m, $k\neq 0$, the latter are separated by additional antimony layers.[32] These phases are accessible as bulk material, however, the long-range ordering of the building blocks can be limited and both stacking disorder as well as varying site occupancies have been described.[31,33,34] These effects probably depend on the exact composition and thermal treatment.

Although frequently disordered, the thermodynamically stable phases contain distorted rocksalt-type slabs rather similar to metastable crystalline phase-change materials and exhibit a similar chemical composition. However, PCMs fortunately do not adopt the thermodynamically stable structures during write-erase cycles. The present study on GeTe-rich bulk samples emphasizes the role of microstrain regarding the inhibition of the cubic-to-rhombohedral phase transition. Mechanical stress as a consequence of the phase transitions influences the kinetics, impedes long-range ordering, and may be important in phase change devices as well.

II. EXPERIMENTAL DETAILS

A. Synthesis

Bulk samples of $Ge_{0.8}Sb_{0.2}Te$ (=Ge_4SbTe_5, $GeTe:Sb_2Te_3:Sb_2=24:2:1$), $Ge_{0.7}Sb_{0.2}Te$ ($GeTe:Sb_2Te_3=7:1$), and $Ge_{0.8}Sb_{0.13}Te$ ($GeTe:Sb_2Te_3=12:1$) were prepared by melting stoichiometric amounts of the pure elements Ge (99.999%, Sigma Aldrich), Sb (99.999%, Smart Elements), and Te (99.999%, Alfa Aesar) in sealed silica glass ampoules under argon atmosphere at 950 °C (~2 h). After quenching to room temperature in water, the samples were annealed at 500 °C ($Ge_{0.8}Sb_{0.13}Te$) or 550 °C ($Ge_{0.8}Sb_{0.2}Te$, $Ge_{0.7}Sb_{0.2}Te$) for 20 h in a tube furnace and quenched in water again. Some samples of $Ge_{0.8}Sb_{0.13}Te$ were ground and separated into fractions with different grain sizes by sieving and subsequently annealed under Ar as described below. These samples were not ground again after annealing and no sintering was observed.

B. Scanning electron microscopy and chemical analysis

Images of the samples were recorded using JSM-6500F (Jeol, USA) scanning electron microscope (SEM) equipped with an energy-dispersive x-ray (EDX) detector (model 7418, Oxford Instruments, Great Britain). The composition of the bulk samples was confirmed by EDX spectroscopy. All analyses of $Ge_{0.7}Sb_{0.2}Te$ and $Ge_{0.8}Sb_{0.13}Te$ corresponded to the stoichiometry of the weighted sample within an error limit of 2–4 at. %. For the analysis of the single crystal from a heterogeneous sample with the nominal composition $Ge_{0.8}Sb_{0.2}Te$ (see below), three-point measurements were averaged.

C. X-ray diffraction

X-ray powder patterns were recorded on a Huber G670 Guinier camera equipped with a fixed imaging plate and integrated read-out system using Cu $K\alpha 1$ radiation (Ge monochromator, $\lambda=1.54051$ Å) in Guinier geometry. Specimens were prepared by fixing powdered specimens on Mylar foils using silicone grease. Lattice parameters were determined by pattern fitting (Rietveld method) using the program TOPAS.[35] Temperature-dependent powder diffraction experiments were done on a STOE Stadi P powder diffractometer equipped with an imaging plate system using Mo $K\alpha 1$ radiation (Ge monochromator, $\lambda=0.71093$ Å) in Debye-Scherrer geometry. Powdered specimens were filled into silica glass capillaries with 0.3 mm diameter and sealed with silicone grease under argon atmosphere. During measurement the samples were heated up to 600 °C in a graphite furnace and then cooled to room temperature.

Irregularly shaped crystals obtained by crushing a quenched sample of Ge_4SbTe_5 were checked for quality by Laue photographs on a Buerger precession camera after mounting them on glass fibers. Intensity data were collected on a Nonius-Kappa CCD diffractometer using Mo $K\alpha$ radiation (graded multilayer x-ray optics, $\lambda=0.71093$ Å). Semiempirical absorption corrections based on equivalent reflections[36] were applied before structure refinements with SHELX.[37] Details concerning the data collection and refinement are summarized in Tables I and II.[38]

D. Transmission electron microscopy

The samples were finely dispersed in ethyl alcohol suspension and subsequently dispersed on copper grids coated with holey carbon film. The grids were mounted on a double tilt holder with a maximum tilt angle of 30°. Selected-area electron diffraction (SAED) and high-resolution transmission electron microscopy (HRTEM) were carried out on a FEI

TABLE I. Crystal data and refinement details for $Ge_{0.7}Sb_{0.2}Te$.

Formula	$Ge_{0.7}Sb_{0.2}Te$
Molar mass in g mol^{-1}	204.7 g/mol
Crystal system	Trigonal
Space group	$R3m$
Cell parameters in Å	a=4.237(3), c=10.29(1)
Cell volume in Å^3	160.0(2)
Formula units/cell	3
X-ray density in g cm^{-3}	6.314
Abs. coefficient in mm^{-1}	25.60
F(000)	253.8
Crystal size in mm^3	0.03×0.03×0.02
Diffractometer	Nonius Kappa-CCD
Radiation, monochromation	Mo $K\alpha$ (λ=0.71073 Å), graded multilayer x-ray optics
Temperature in K	293(2)
2θ range in deg	11.8–66.3
Total no. of reflections	2240
Independent/observed reflections	99/97
Refined parameters	12
GOF	1.090
R values [$I>2\sigma(I)$]	$R1$=0.0319, $wR2$=0.0750
All data	$R1$=0.0329, $wR2$=0.0764
Max./min. residual electron density in eÅ^{-3}	1.085/−1.567

Titan 80–300 equipped with a field emission gun operating at 300 kV. The images were recorded using a Gatan UltraScan 1000 (2k×2k) camera.

III. RESULTS AND DISCUSSION

A. Electroneutrality and phase separation

According to literature,[24–26] a cubic B1-type phase $Ge_{0.8}Sb_{0.2}Te$ (=Ge_4SbTe_5, $GeTe:Sb_2Te_3:Sb_2$=24:2:1) can be obtained as bulk material. However, we were not able to obtain single-phase samples with this composition. Instead, x-ray powder diffraction patterns of various both quenched and annealed samples always indicated formation of elemental Ge in the samples. Optical microscopy on polished samples shows dark spots due to Ge precipitation. In contrast to thin-film samples, where a B1-type material without cation vacancies has been reported with anion to cation ratio 1,[24–26] our results are in accordance with the ternary phase diagram. Metastable phases are, of course, not well described by phase diagrams, however, the latter indicate the precipitation of Ge, which can be explained regarding the charge balance in a semiconductor with formal oxidation states Ge^{II}, Sb^{III}, and Te^{-II}. For $Ge_{0.8}Sb_{0.2}Te$, the charge balance between anions (−2) and cations (average charge +2.2) does not correspond to a valence compound whereas all stable phases on the pseudobinary section $(GeTe)_n(Sb_2Te_3)_m$ are valence compounds per definition. Hence, the electron count suggests that $Ge_{0.8}Sb_{0.2}Te$ is expected to be metastable against phase separation. Electroneutrality can, in principle, be achieved by precipitation of either Ge or Sb. The Ge precipitation observed is easy to detect as Ge crystallizes in a cubic diamond type ($Fd\bar{3}m$) which does not allow coherent intergrowth. In contrast, spinodal Sb exsolution might be kinetically favored (but has not been observed for this composition) because its layerlike gray arsenic-type structure (A7, $R\bar{3}m$) is closely related to the structure of stable trigonal germanium antimony tellurides. The similar metrics perpendicular to the rhombohedral axis (differences <2%) allows coherent intergrowth that may even lead to new long-range ordered intergrowth phases, especially for higher Sb contents as in $Ge_{1.57}Sb_{2.43}Te_5 \cdot Sb_8$.[32]

From these considerations, single-phase samples require at least a composition on the pseudobinary section

TABLE II. Atom coordinates, occupation factors, and diplacement factors (in Å^2) $Ge_{0.7}Sb_{0.2}Te$.

Atom	Wyckoff site	$x=y$	z	$f.o.f.$	U_{eq}	$U_{11}=U_{22}$	U_{33}	$U_{23}=U_{13}$	$U_{12}=1/2U_{11}$
Ge/Sb	3a	0	0.4808(3)	Ge 0.70 Sb 0.20	0.0221(7)	0.0214(11)	0.024(2)	0	0.0107(5)
Te	3a	0	0	1	0.0290(4)	0.0284(8)	0.0302(18)	0	0.0142(4)

$GeTe$-Sb_2Te_3, e.g., $Ge_{0.7}Sb_{0.2}Te$ ($GeTe:Sb_2Te_3=7:1$) and $Ge_{0.8}Sb_{0.13}Te$ ($GeTe:Sb_2Te_3=12:1$). In any case, thermal treatment of these samples does not lead to the formation of Sb or Ge but rather to separation into interrelated ordered compounds on the mentioned line. However, in a (pseudo)cubic B1 structure, the Sb content of these phases leads to cation vacancies ($Ge_{1-x}Sb_{2x/3}\square_{x/3}Te$).

B. Average crystal structure of the quenched samples

Quenched bulk samples with the composition $Ge_{0.8}Sb_{0.2}Te$ ($=Ge_4SbTe_5$, $GeTe:Sb_2Te_3:Sb_2=24:2:1$) contain precipitated Ge (as mentioned above), however, small single crystals of a ternary phase can be isolated from the ingots. To confirm the average structure of the (pseudo)cubic phase we performed single-crystal diffraction experiments on such metastable single crystals. EDX spectroscopy yields a composition $Ge_{0.71(1)}Sb_{0.195(10)}Te$ which corresponds very well to an electroneutral formula $Ge_{0.7}Sb_{0.2}Te$ and indicates phase separation according to $Ge_{0.8}Sb_{0.2}Te \rightarrow Ge_{0.7}Sb_{0.2}Te + 0.1$ Ge. At first sight, the average structure of $Ge_{0.7}Sb_{0.2}Te$ is a B1 rocksalt type with a lattice constant of $a_c = 5.991(1)$ Å (the subscript c denotes the cubic setting). Since such compounds can be regarded as a Sb-doped variant of GeTe, a rhombohedral structure model has been suggested for the related phase $Ge_8Sb_2Te_{11}=Ge_{0.72}Sb_{0.18}Te$ (Ref. 22) in analogy to the displacive phase transition between β and α GeTe (Ref. 23), which involves a symmetry reduction from $Fm\bar{3}m$ to $R3m$. A simple distortion of the cF lattice along $\langle 111\rangle_c$ yields a centrosymmetric hR lattice. In single crystals, such a *translationengleiche* group-subgroup relationship of index 4 ($t4$) usually involves fourfold twinning. The formation of a polar layered GeTe-type structure requires further symmetry reduction from $R\bar{3}m$ to $R3m$ ($t2$), leading to additional inversion twinning. Both $R\bar{3}m$ and $R3m$ contain two independent atom positions corresponding to the anion (Te) and cation (Ge+Sb+vacancies) sublattices, respectively. Whereas the deviation from the cubic metrics is relatively small, the trigonal symmetry of twin domains and their relative orientation are quite obvious in SEM images of fragments from the ingot as shown in Fig. 1.

Structure refinements have been performed using different models in space groups $Fm\bar{3}m$, $R\bar{3}m$, and $R3m$, respectively. In order to comply with the cubic Laue symmetry of the diffraction data as well as with group-subgroup relationships, fourfold pseudomerohedral twinning for the rhombohedral models must be considered. The relative volume fractions of the four domains refined to 0.241(4):0.251(4):0.265(4):0.243(4). Additional inversion twinning in the case of $R3m$ could not be taken into account as refinements became unstable, however, Flack parameters indicate that inversion twinning is present. In preliminary refinements, full Ge/Sb occupancy has been assumed for cation as well as anion positions for better comparison of different models. Although at first glance the refinement assuming a B1-type rocksalt structure seems satisfactory [$Fm\bar{3}m$, 38 independent data, 3 parameters; $R1(\text{all})=0.062$], symmetry reduction and accounting for twinning improve the residuals significantly

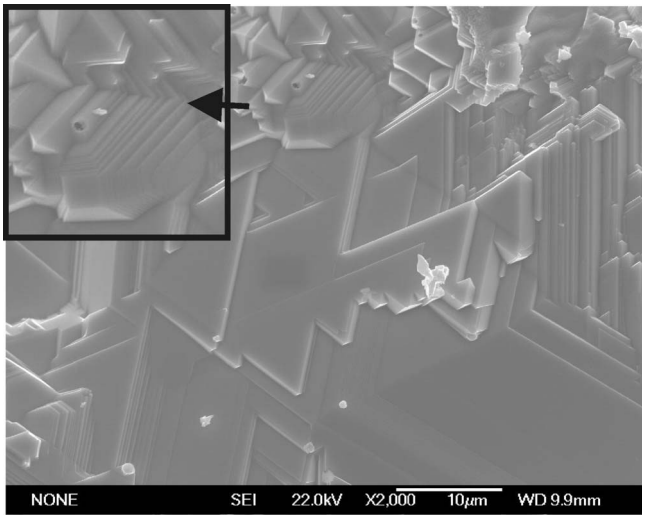

FIG. 1. SEM image of a fragment of an ingot with the composition $Ge_{0.7}Sb_{0.2}Te$; the trigonal morphology of plate-shaped domains and their multiple twinning to form pseudocubic arrangements (see magnified inset) is easily seen.

[$R\bar{3}m$: 99 independent data, 8 parameters, $R1(\text{all})=0.045$; $R3m$: 99 independent data (Friedel pairs averaged), 11 parameters, $R1(\text{all})=0.033$]. Although the final model in $R3m$ has more parameters, the improvement of the data fit is statistically significant. This result confirms the reasonable assumption of a GeTe-type structure. If the Ge and Sb fractions on the cation site are refined with the constraint of total charge neutrality [2 sof(Ge)+3 sof(Sb)=2 sof(Te)], the resulting composition is $Ge_{0.689(1)}Sb_{0.207(1)}Te$. This is consistent with the EDX result, however, in combination with the twin fractions the refinement requires strong damping. Therefore, the slightly idealized composition $Ge_{0.7}Sb_{0.2}Te$ was fixed in the final refinement. As the metrical rhombohedral distortion cannot be quantified from a twinned crystal (which apparently exhibits the cubic metrics), the lattice parameters used for the calculation of interatomic distances and angles were determined from powder data (see below). Crystallographic details are given in Table I, atom positions, site occupancies, and displacement parameters are given in Table II.

In the final GeTe-type structure model (cf. Fig. 2), the coordination octahedron around Ge/Sb is distorted, resulting in three short distances Ge/Sb-Te [2.879(2) Å] and three long distances Ge/Sb-Te [3.105(2) Å] with angles Te-Ge/Sb-Te of 94.76(7)° and 86.05(7)° at the cation. Thus, the structural deviation from the B1 type is much larger than the deviation from the cubic metrics. The distances and angles correspond well to the values for $Ge_8Sb_2Te_{11}$ ($R3m$, $a_h = 4.203$ Å, $c_h = 10.458$ Å at 92 K; the subscript h denotes hexagonal setting) that were obtained by Rietveld refinement on powder data (distances Ge/Sb-Te: 2.883 and 3.101 Å, angles Te-Ge/Sb-Te: 93.6° and 85.3°).[22]

C. *In situ* temperature-dependent powder diffraction study

The powder patterns of quenched GeTe-rich phases with electroneutral compositions such as $Ge_{0.7}Sb_{0.2}Te$ and

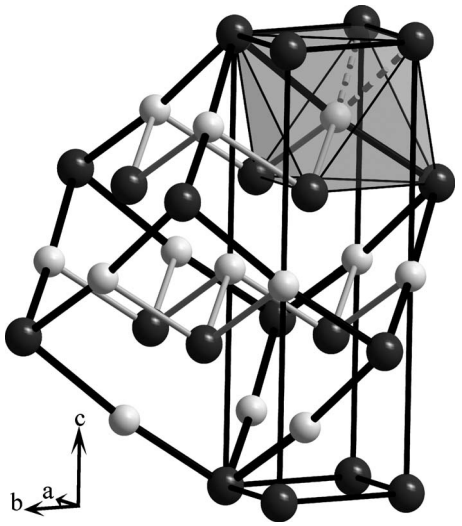

FIG. 2. Representation of the crystal structure of quenched $Ge_{0.7}Sb_{0.2}Te$ (white spheres: cation position with Ge, Sb, and vacancy occupation, dark spheres: Te): both the rhombohedral (hexagonal setting, upright) and the pseudocubic rocksalt-type unit cells are outlined, GeTe-type layers are indicated by interconnection of the atoms with the shortest interatomic distances, some of the longer interatomic distances are also indicated (gray fragmented "bonds" that highlight the pseudo-octahedral coordination of the cations).

$Ge_{0.8}Sb_{0.13}Te$ indicate single-phase products with pseudocubic metrics consistent with the single-crystal experiment, the a_c lattice parameter being approximately 5.99 Å, corresponding to $a_h \approx 4.235$ Å and $c_h \approx 10.37$ Å (again, the indices c and h indicate cubic and hexagonal setting, respectively). The slight rhombohedral distortion along $[111]_c$ is manifested in the anisotropic peak broadening of the pseudocubic reflections (see below). It corresponds to approximate rhombohedral lattice parameters $a_h = 4.237$ Å and $c_h = 10.29$ Å for $Ge_{0.7}Sb_{0.2}Te$ and $a_h = 4.237$ Å and $c_h = 10.36$ Å for $Ge_{0.8}Sb_{0.13}Te$ (for comparison: GeTe:[23] $a_h = 4.164$ Å and $c_h = 10.692$ Å). *In situ* temperature-dependent powder diffraction experiments prove that this structural state is metastable. The kinetic stabilization of the pseudocubic phase is more pronounced for $Ge_{0.8}Sb_{0.13}Te$ (cf. Fig. 3), therefore we chose this sample for a detailed investigation. Upon heating, structural changes are observed as reported earlier.[22] The anisotropically broadened reflections of $Ge_{0.8}Sb_{0.13}Te$ split into the typical strong reflections corresponding to a clearly rhombohedral GeTe-type pattern at approximately 325 °C. As detailed below, this is the average structure of a disordered superstructure phase that includes blocks of various GeTe-rich compounds $(GeTe)_n(Sb_2Te_3)$. Clearly visible superstructure reflections are not expected as no long-time annealing has been applied. A second phase transition to a phase with regular cubic metrics occurs at about 475 °C. Peak integrals of this cubic high-temperature phase and the quenched (pseudo)cubic phase correspond well, but the absence of anisotropic broadening indicates a genuine stable rocksalt-type phase at high temperatures. Upon slow cooling of the sample to room temperature, the more or less disordered block structure with pronounced

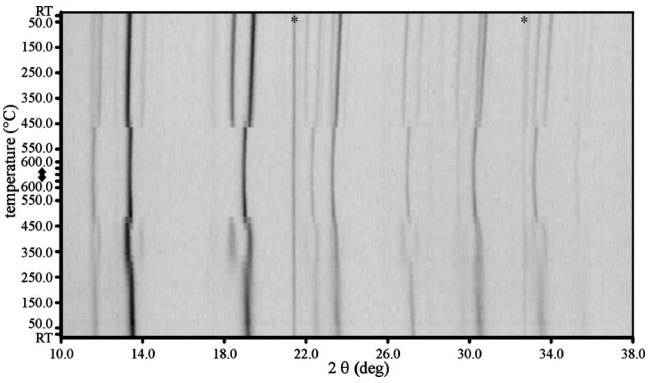

FIG. 3. Temperature-programmed powder diffraction experiment (Mo $K\alpha 1$ radiation) of a quenched sample $Ge_{0.8}Sb_{0.13}Te$ (from bottom to top, heating and cooling ramp 5 °C/min). At 600 °C, several patterns were recorded and later added to obtain more precise lattice parameters of the high-temperature phase. One reflection from the furnace material is indicated by an asterisk.

rhombohedral distortion is obtained instead of a (pseudo)cubic state. Weak additional reflections of a phase very similar to GeTe were sometimes observed.

D. Transmission electron microscopy

HRTEM images of a $Ge_{0.8}Sb_{0.13}Te$ specimen quenched from 500 °C show a disordered domain structure with parquetlike appearance (cf. Fig. 4, top). It can be interpreted in terms of planar defects, and similar effects have been reported for copper gallium chalcogenides.[39] From the structures of the corresponding stable phases as well as from theoretical calculations[7,17,28,33,34,40–42] it seems obvious that cation vacancies tend to arrange as planar defect layers accompanied by local distortions in the crystal structure. In fact, the van der Waals gaps between the rocksalt-type blocks in $(GeTe)_n(Sb_2Te_3)$ phases can be viewed as defect layers, if the shift between adjacent Te atom layers is considered as a relaxation. The partial cation defect ordering in $Ge_{0.8}Sb_{0.13}Te$ extends in planes $\|\{111\}_c$, i.e., parallel to the single hexagonal atom layers of the cubic *ABC* stacking sequence. Interpenetrating nanodomains with different orientations inhibit long-periodic ordering of the layer faults and on average, the resulting disordered structure maintains cubic metrics (see below). The domains are much smaller than in $Ge_{0.7}Sb_{0.2}Te$ (cf. Fig. 2), and crystals of $Ge_{0.8}Sb_{0.13}Te$ would not be suitable for twin refinements as the x-rays' length of coherence exceeds the domain size. Therefore, the elementary mesh of the $h\bar{h}l_c$ electron diffraction pattern (cf. Fig. 5, bottom) exhibits no significant deviation from the expected $1/\sqrt{2}$ lattice parameter ratio. The elongation of the Bragg maxima along $\langle 111 \rangle$ can be attributed to local rhombohedral distortion. The statistical distribution of the planar defects leads to diffuse lines interconnecting the Bragg intensities along $\langle 111 \rangle$, consistent with the Fourier transform of the HRTEM image.

After further annealing of the samples previously quenched from 500 °C (stability region of the cubic high-temperature phase) at 400 °C (below the transition temperature to the cubic high-temperature modification) for 20 h, the

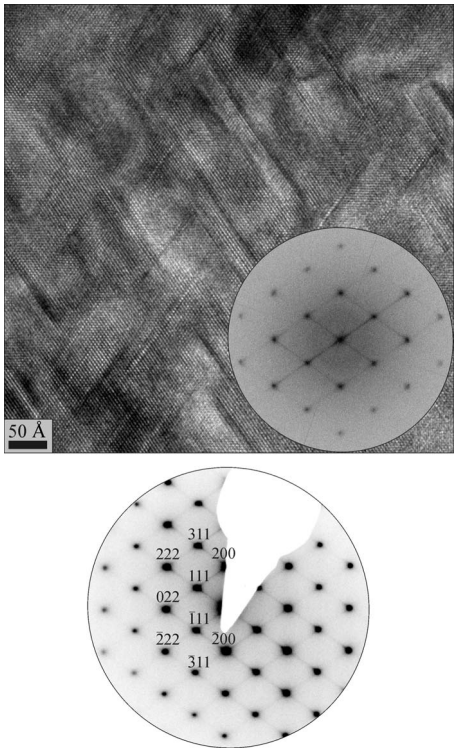

FIG. 4. HRTEM image of a $Ge_{0.8}Sb_{0.13}Te$ specimen as quenched from 500 °C (top, inset: Fourier transform) and the corresponding SAED pattern (bottom, indices of some Bragg positions are given).

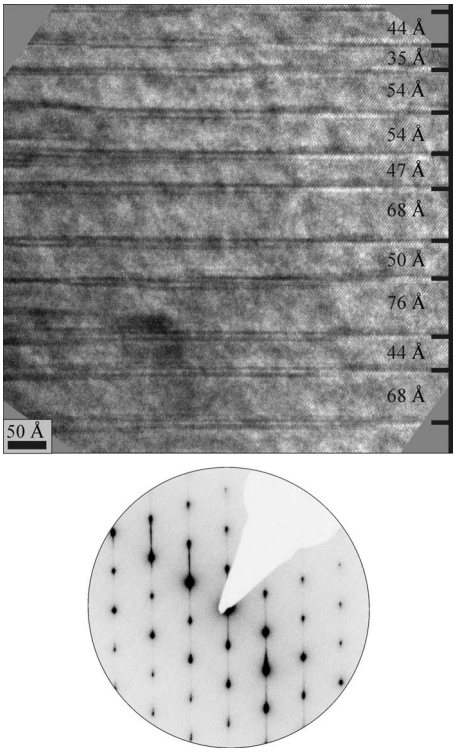

FIG. 5. HRTEM image of a $Ge_{0.8}Sb_{0.13}Te$ specimen annealed at 400 °C for 20 h and subsequently quenched (top, the spacings of cation defect layers are indicated, they yield an average of 54 Å) and the corresponding SAED pattern (bottom).

planar defects adopt a strongly preferred orientation perpendicular to the $[001]_h$ direction of a rhombohedral GeTe-type unit cell (cf. Fig. 5, $[001]_h$ corresponds to one of the $\langle 111\rangle_c$ directions, *h* and *c* indicate hexagonal and cubic setting, respectively). The defect layers appear as rather broad lines as the relaxation around them continues into several atom layers of the rocksalt-type slabs. As measured in HRTEM images, the average distance between the defect layers is about 54 Å, but in contrast to a well-defined superstructure they are not arranged periodically and their distance varies up to 30 Å around the average value. Similar one-dimensional disorder has been reported, for example, for the phases $GeSb_2Te_4$, $Ge_2Sb_2Te_5$, or $Ge_3Sb_2Te_6$.[33,34] Consequently, the SAED patterns show diffuse streaks along c_h^*.

An idealized hypothetical superstructure corresponding to the given composition can be derived by homology principles as described in detail in the literature.[28,31] The number of cation defects and thus the frequency of van der Waals gaps depends on the Sb content and, in this case, leads to rather thick rocksalt-type slabs. For the composition $Ge_{0.8}Sb_{0.13}Te=(GeTe)_{12}(Sb_2Te_3)$, an 87*R* type with a c_h lattice constant of approximately 165.3 Å is expected as the average thickness for two-dimensional hexagonal atom layers in these long periodically ordered structures is about 1.9 Å. In such an 87*R*-type structure, one c_h translation period contains three rocksalt-type slabs comprising 29 atom layers each. Consequently, the distance between the van der Waals gaps, i.e., the cation defect layers, is expected to be 55.1 Å. This agrees well with the experimentally determined average value, although this is just an approximation as a certain degree of GeTe exsolution cannot be excluded.

E. Influence of the powder-particle size on the establishment of the rhombohedral distortion

The transformation between the quenched pseudocubic state and the rhombohedral superstructure phase depends on time and temperature. The pseudocubic state itself differs from the cubic high-temperature phase by the formation of a GeTe-type structural distortion and by formation of the planar defect layers $\parallel\{111\}_c$, which both can be expected to drive a rhombohedral distortion of the lattice metrics. However, the formation of the rhombohedrally distorted GeTe-type state is realized in twin domains differing by the orientation of the $[001]_h$ direction corresponding to different $\langle 111\rangle_c$ directions. In this state, the planar defect layers are aligned perpendicular $[001]_h$ of the corresponding rhombohedral domain. Within the small-domain-sized microstructure, each domain is hindered to establish its stress-free rhombohedrally distorted metrics (equilibrium lattice parameters), and the metrical misfit between the different domains leads to locally varying deviations from the equilibrium lattice parameters to pseudocubic ones (microstrain accompanied by microstress). Depending on the domain size and actual domain microstructure, this either leads to an incomplete rhombohedral splitting or merely to the anisotropic microstrain broadening of the reflections in a powder diffraction pattern that would be expected for a cubic phase.

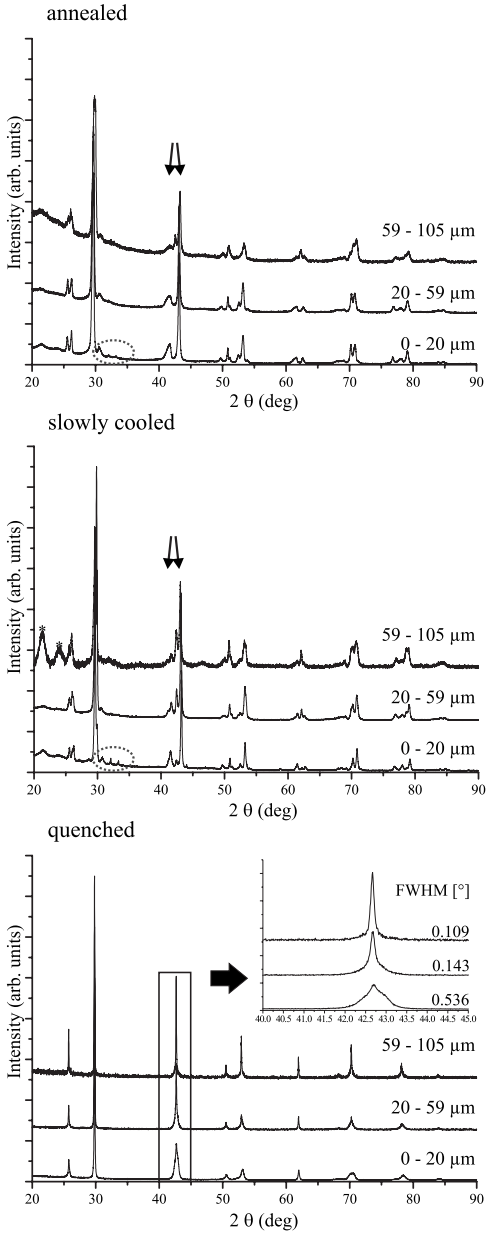

FIG. 6. Powder diffraction patterns of fractions of $Ge_{0.8}Sb_{0.13}Te$ samples with grain sizes 0–20 μm, 20–59 μm, and 59–105 μm: quenched from 500 °C (bottom, with anisotropic peak broadening depending on the grain size, inset: 220_c reflection and its full width at half maximum), slowly cooled from 500 to 250 °C (middle, the asterisks indicate diffracted intensity from the sample support) and quenched after annealing at 400 °C for 20 h (top). The slowly cooled and annealed samples show rhombohedral reflection splitting (indicated by arrows for the 104_h and 110_h reflections) and superstructure reflections (marked for the batches with the smallest grain sizes by dotted ellipses at an exemplary position).

Indeed the powder diffraction patterns (Fig. 6, bottom) of the quenched samples exhibit anisotropic broadening with the hhh_c (111 and 222) reflections being very broad and the $h00_c$ (200 and 400) reflections being narrowest. This anisotropy of the broadening reflects the fact that the $h00_c$ reflections do not split upon a rhombohedral distortion, whereas for hhh_c this splitting will be largest (e.g., 003_h and 101_h originating from 111_c). In the experimental pattern (Fig. 6, bottom), the broadening is highlighted for the strong 220_c reflection which formally splits into the 104_h and 110_h reflections. The order dependence of the line broadening of the hhh_c reflections in Williamson-Hall plots[43] (not shown) clearly confirms the microstrain character of the line broadening as expected for varying d spacings in the specimen. However, a quantitative evaluation of the line broadening is complicated by coherent-diffraction effects between the small domains and by the stacking faults.[44–46] Moreover, the planar defect layers may also lead to layer-fault-induced line broadening, however, this is apparently not large in the present case.

The free surface, which depends on the size of the powder particles, is a decisive factor concerning possible relaxation of the stresses in domains which, in turn, allows for better establishment of the rhombohedral distortion. Therefore, powder samples of $Ge_{0.8}Sb_{0.13}Te$ were separated into fractions with defined grain sizes of 0–20 μm, 20–59 μm, and 59–105 μm before they were annealed in the stability region of the cubic modification (at 500 °C) and subsequently quenched in water. No further grinding was applied; therefore, the peak shapes are not biased by grinding effects which may otherwise have a strong influence. In fact, the powder batches with the smallest particle size (which is definitely larger than the domain size, cf. Fig. 4) exhibit the largest line broadening with respect to an unbroadened cubic pattern, and are thus closest to the rhombohedral pattern (Fig. 6, bottom). Particle-size broadening can be neglected as the reflections that do not split in the rhombohedral system remain sharp.

The pseudocubic rhombohedral state with more or less pronounced microstrain broadening is kinetically stable at ambient temperature. However, upon annealing (400 °C for 20 h) the domains of the pseudocubic state coarsen and optimize their mutual arrangement. This way the stress-free rhombohedral lattice parameters are approached (similar to the observations in the course of the high-temperature powder diffraction experiments, see above). At the same time the defect-layers reorient perpendicular to the $[001]_h$ direction of the larger domains and order in a long-range fashion so that superstructure reflections appear. This occurs most readily for the smallest powder-particle-size batch, where the superstructure reflections are best visible (Fig. 6, top). Apparently, the free surfaces enhance the coarsening and the defect-layer ordering, similar to abnormal grain growth.[47] In additional experiments, similar powder batches of $Ge_{0.8}Sb_{0.13}Te$ were slowly cooled from 500 to 250 °C and then quenched by removing them from the furnace. The changes observed in the powder patterns of these samples are even more pronounced than for annealed samples.

In the course of the present investigations, two different ternary phases have been observed: the cubic high-temperature phase and the metastable disordered pseudocubic or clearly distorted phase with a GeTe-type basic structure. A long-range ordered phase containing periodically arranged planar defect layers would constitute a third phase that has not been observed in its ideal state. We note that the pseudocubic GeTe-type state and the rhombohedrally distorted GeTe-type states without clear indication of long-

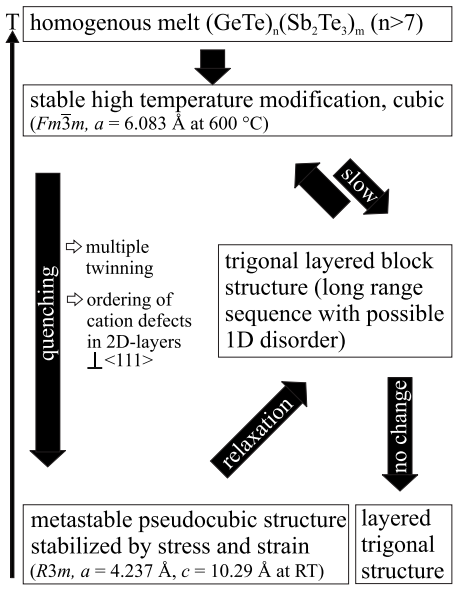

FIG. 7. Phase relations and transformations between the cubic high-temperature phase, the metastable pseudocubic or rhombohedral phase, and the stable trigonal layered superstructure of GeTe-rich GST materials as observed for bulk samples.

range order should be regarded as the same phase, however, with different microstructures. Indeed, the lattice parameters observable by diffraction methods are sometimes determined by the microstructure, e.g., in Pd_6B.[48] However, it is impossible to clearly distinguish a long-range ordered phase with a certain amount of disorder from a GeTe-type phase with defect layers that does not exhibit long-range periodicity.

IV. CONCLUSIONS

The present study shows that bulk samples of quenched GeTe-rich GST materials exhibit phase relationships and transformations (cf. Fig. 7) between metastable states and stable trigonal phases that are very similar to those observed in thin films of phase-change materials on rewritable data-storage media.[22] If the cubic high-temperature phase is quenched, the phase transition to a rhombohedral phase leads to twin domains, which has been shown by HRTEM as well as by the first single-crystal structure refinement of a metastable GST phase in its pseudocubic state. Temperature-dependent powder diffraction experiments have clearly revealed that in this case the formation of the stable ordered phases is inhibited by stress that arises from the formation of twin domains due to the anisotropic distortion associated with the formation of the rhombohedral phase. Thus, the realignment into areas with long-periodic parallel defect layers is hindered in large powder particles or compact bulk material, whereas the necessary relaxation occurs more readily in small powder particles. Surface effects may also play a role. Summing up, the transition kinetics is strongly affected by stress effects.

In PCM data-storage devices, only small regions of thin films are actually melted and quickly recrystallized (i.e., quenched) to code information, hence, the surrounding matrix can lead to anisotropic stress.[49–51] Pressures during the write-erase cycle have been estimated to reach up to several gigapascal.[52–54] A strong mechanical force, which results mainly from interactions between substrate and capping cannot be neglected within the phase-change material itself. In this context, our results show that stress and strain effects in GST phases are not only important for the write-erase cycle but also with respect to the kinetic inhibition of the formation of the stable trigonal phases. Thus, they play a decisive role in PCMs and are not only interesting with respect to adhesion between the storage layer and its surrounding. Comparable strain effects have been investigated, for example, in ferroelectric or ferroelastic materials,[55,56] metals,[57,58] and alloys,[59] and shown to influence the electrical behavior of perovskites.[60] Concerning phase-change materials, most research has concentrated on the amorphous-crystalline transitions so far. However, to understand their crystal chemistry and physics, it is also essential to take into account the transitions between metastable and stable crystalline modifications, especially since the latter involve the impetus of thermodynamics. This insight into the interplay of kinetics and thermodynamics of GST materials might also be interesting with respect to their potential thermoelectric properties.[30] Therefore, it seems promising to further investigate this relationship.

ACKNOWLEDGMENTS

The authors thank Peter Mayer (LMU Munich) for the single-crystal data collection, Christian Minke (LMU Munich) for SEM operation and EDX analyses. Thomas Woehrle (MPI-MF, Stuttgart) for the optical microscopy on polished cross-sections, and Thomas Miller (LMU Munich) for the temperature-dependent powder diffraction experiments. Furthermore, we are indebted to Eric J. Mittemeijer (MPI-MF, Stuttgart) for providing department facilities and Wolfgang Schnick (LMU Munich) for his generous support of this work. This investigation was funded by the Deutsche Forschungsgemeinschaft (Grant No. OE530/1-1).

*Author to whom correspondence should be addressed. FAX: (+49)89-2180-77440; oliver.oeckler@gmx.de

[1] M. Wuttig and C. Steimer, Appl. Phys. A: Mater. Sci. Process. **87**, 411 (2007).
[2] M. Wuttig, Nature Mater. **4**, 265 (2005).
[3] M. Wuttig and N. Yamada, Nature Mater. **6**, 824 (2007).
[4] A. L. Greer and N. Mathur, Nature (London) **437**, 1246 (2005).
[5] T. Matsunaga and N. Yamada, Jpn. J. Appl. Phys., Part 1 **41**, 1674 (2002).
[6] T. Matsunaga and N. Yamada, Jpn. J. Appl. Phys., Part 1 **43**,

4704 (2004).
[7] L. E. Shelimova, O. G. Karpinsky, P. P. Konstantinov, M. A. Kretova, E. S. Avilov, and V. S. Zemskov, Inorg. Mater. **37**, 342 (2001).
[8] V. I. Kosyakov, V. A. Shestakov, L. E. Shelimova, F. A. Kuznetsov, and V. S. Zemskov, Inorg. Mater. **36**, 1004 (2000).
[9] B. Legendre, C. Hancheng, S. Bordas, and M. T. Clavaguera-Mora, Thermochim. Acta **78**, 141 (1984).
[10] S. Bordas, M. T. Clavaguera-Mora, B. Legendre, and C. Hancheng, Thermochim. Acta **107**, 239 (1986).
[11] A. V. Kolobov, P. Fons, A. I. Frenkel, A. L. Ankudinov, J. Tominaga, and T. Uruga, Nature Mater. **3**, 703 (2004).
[12] A. V. Kolobov, P. Fons, J. Tominaga, and T. Uruga, J. Non-Cryst. Solids **352**, 1612 (2006).
[13] J. Hegedüs and S. R. Elliott, Nature Mater. **7**, 399 (2008).
[14] W. Wełnic and M. Wuttig, Mater. Today **11**, 20 (2008).
[15] D. Lencer, M. Salinga, B. Grabowski, T. Hickel, J. Neugebauer, and M. Wuttig, Nature Mater. **7**, 972 (2008).
[16] T. Matsunaga, R. Kojima, N. Yamada, K. Kifune, Y. Kubota, Y. Tabata, and M. Takata, Inorg. Chem. **45**, 2235 (2006).
[17] Z. Sun, J. Zhou, and R. Ahuja, Phys. Rev. Lett. **96**, 055507 (2006).
[18] T. Matsunaga and N. Yamada, Phys. Rev. B **69**, 104111 (2004).
[19] T. Matsunaga, N. Yamada, and Y. Kubota, Acta Crystallogr., Sect. B: Struct. Sci. **60**, 685 (2004).
[20] M. Wuttig, D. Lüsebrink, D. Wamwangi, W. Wełnic, M. Gilleßen, and R. Dronskowski, Nature Mater. **6**, 122 (2007).
[21] Z. Sun, S. Kyrsta, D. Music, R. Ahuja, and J. M. Schneider, Solid State Commun. **143**, 240 (2007).
[22] T. Matsunaga, H. Morita, R. Kojima, N. Yamada, K. Kifune, Y. Kubota, Y. Tabata, J.-J. Kim, M. Kobata, E. Ikenaga, and K. Kobayashi, J. Appl. Phys. **103**, 093511 (2008).
[23] T. Chattopadhyay, J. X. Boucherle, and H. G. von Schnering, J. Phys. C **20**, 1431 (1987).
[24] J. González-Hernández, E. López-Cruz, M. Yáñez-Limón, D. Strand, B. B. Chao, and S. R. Ovshinsky, Solid State Commun. **95**, 593 (1995).
[25] E. Morales-Sánchez, E. F. Prokhorov, J. González-Hernández, and A. Mendoza-Galván, Thin Solid Films **471**, 243 (2005).
[26] D. Wamwangi, W. K. Njoroge, and M. Wuttig, Thin Solid Films **408**, 310 (2002).
[27] P. F. P. Poudeu and M. G. Kanatzidis, Chem. Commun. (Cambridge) **2005**, 2672.
[28] L. E. Shelimova, O. G. Karpinsky, M. A. Kretova, V. I. Kosyakov, V. A. Shestakov, V. S. Zemskov, and F. A. Kuznetsov, Inorg. Mater. **36**, 768 (2000).
[29] K. Kifune, Y. Kubota, T. Matsunaga, and N. Yamada, Acta Crystallogr., Sect. B: Struct. Sci. **61**, 492 (2005).
[30] P. P. Konstantinov, L. E. Shelimova, E. S. Avilov, M. A. Kretova, and V. S. Zemskov, Inorg. Mater. **37**, 662 (2001).
[31] M. N. Schneider and O. Oeckler, Z. Anorg. Allg. Chem. **634**, 2557 (2008).
[32] M. N. Schneider, M. Seibald, and O. Oeckler, Dalton Trans. **2009**, 2004.
[33] S. Kuypers, G. van Tendeloo, J. van Landuyt, and S. Amelinckx, J. Solid State Chem. **76**, 102 (1988).
[34] B. J. Kooi and J. T. M. De Hosson, J. Appl. Phys. **92**, 3584 (2002).
[35] A. Coelho, TOPAS-ACADEMIC, V. 4.1, Coelho Software, Brisbane (2007).
[36] G. M. Sheldrick, SADABS, Version 2.10, Bruker AXS Inc., Madison, Wisconsin (2001).
[37] G. M. Sheldrick, Acta Crystallogr., Sect. A: Found. Crystallogr. **64**, 112 (2008).
[38] Further details may be obtained from Fachinformationszentrum Karlsruhe, 76344 Eggenstein-Leopoldshafen, Germany [fax: (+49)7247–808–666; e-mail: crysdata@fiz-karlsruhe.de, http://www.fiz-karlsruhe.de /request_for_deposited_data.html] on quoting the reference number CSD-420919.
[39] L. Kienle, V. Duppel, A. Simon, and H. J. Deiseroth, Z. Anorg. Allg. Chem. **629**, 1412 (2003).
[40] B. J. Kooi, W. M. G. Groot, and J. T. M. De Hosson, J. Appl. Phys. **95**, 924 (2004).
[41] Y. J. Park, J. Y. Lee, and Y. T. Kim, Appl. Surf. Sci. **252**, 8102 (2006).
[42] Y. J. Park, J. Y. Lee, and Y. T. Kim, Appl. Surf. Sci. **253**, 714 (2006).
[43] G. K. Williamson and W. H. Hall, Acta Metall. **1**, 22 (1953).
[44] H. Boysen, J. Phys.: Condens. Matter **19**, 275206 (2007).
[45] D. Rafaja, V. Klemm, G. Schreiber, M. Knapp, and R. Kuzel, J. Appl. Crystallogr. **37**, 613 (2004).
[46] A. Leineweber, E. J. Mittemeijer, M. Knapp, and C. Baehtz, Philos. Mag. **87**, 1821 (2007).
[47] C. V. Thompson, H. J. Frost, and F. Spaepen, Acta Metall. **35**, 887 (1987).
[48] T. G. Berger, A. Leineweber, E. J. Mittemeijer, C. Sarbu, V. Duppel, and P. Fischer, Z. Kristallogr. **221**, 450 (2006).
[49] A. V. Kolobov, Nature Mater. **7**, 351 (2008).
[50] I. M. Park, J. K. Jung, S. O. Ryu, K. J. Choi, B. G. Yu, Y. B. Park, S. M. Han, and Y. C. Joo, Thin Solid Films **517**, 848 (2008).
[51] W. K. Njoroge, H.-W. Wöltgens, and M. Wuttig, J. Vac. Sci. Technol. A **20**, 230 (2002).
[52] Q. Guo, M. H. Li, Y. Li, L. P. Shi, T. C. Chong, J. A. Kalb, and C. V. Thompson, Appl. Phys. Lett. **93**, 221907 (2008).
[53] T. P. L. Pedersen, J. Kalb, W. K. Njoroge, D. Wamwangi, M. Wuttig, and F. Spaepen, Appl. Phys. Lett. **79**, 3597 (2001).
[54] J. Kalb, F. Spaepen, T. P. L. Pedersen, and M. Wuttig, J. Appl. Phys. **94**, 4908 (2003).
[55] T. Lookman, S. R. Shenoy, K. Ø. Rasmussen, A. Saxena, and A. R. Bishop, Phys. Rev. B **67**, 024114 (2003).
[56] L. W. Chang, M. McMillen, and J. M. Gregg, Appl. Phys. Lett. **94**, 212905 (2009).
[57] B. Clausen, C. N. Tomé, D. W. Brown, and S. R. Agnew, Acta Mater. **56**, 2456 (2008).
[58] Z. Budrovic, H. van Swygenhoven, P. M. Derlet, S. van Petegem, and B. Schmitt, Science **304**, 273 (2004).
[59] S. A. Kibey, L. L. Wang, J. B. Liu, H. T. Johnson, H. Sehitoglu, and D. D. Johnson, Phys. Rev. B **79**, 214202 (2009).
[60] K. H. Ahn, T. Lookman, and A. R. Bishop, Nature (London) **428**, 401 (2004).